

University of Arkansas, Fayetteville

ScholarWorks@UARK

Biological and Agricultural Engineering
Undergraduate Honors Theses

Biological and Agricultural Engineering

5-2023

Preparing Homogenous Composites of Collagen and Cellulose Nanocrystals for Tissue Engineering Research

Zachary Stanley

University of Arkansas, Fayetteville

Follow this and additional works at: <https://scholarworks.uark.edu/baeguht>



Part of the [Biological Engineering Commons](#), [Molecular, Cellular, and Tissue Engineering Commons](#), and the [Nanotechnology Commons](#)

Citation

Stanley, Z. (2023). Preparing Homogenous Composites of Collagen and Cellulose Nanocrystals for Tissue Engineering Research. *Biological and Agricultural Engineering Undergraduate Honors Theses* Retrieved from <https://scholarworks.uark.edu/baeguht/94>

This Thesis is brought to you for free and open access by the Biological and Agricultural Engineering at ScholarWorks@UARK. It has been accepted for inclusion in Biological and Agricultural Engineering Undergraduate Honors Theses by an authorized administrator of ScholarWorks@UARK. For more information, please contact scholar@uark.edu, uarepos@uark.edu.


**Preparing Homogenous Composites of Collagen and Cellulose Nanocrystals
for Tissue Engineering Research**

Zachary D. Stanley


Biological Engineering Program
Biological and Agricultural Engineering Department
College of Engineering
University of Arkansas
Undergraduate Honors Thesis

ADVISORY AND COMMITTEE SIGNATURE PAGE

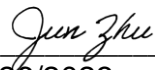
This thesis has been approved by the Biological and Agricultural Engineering Department for submission to the College of Engineering and Honors College at the University of Arkansas.



5/2/2023 (Signature and Date)
BENG Honors Advisor



Date) (Signature and
Honors Committee Member



4/26/2023 (Signature and Date)
Honors Committee Member

ABSTRACT

Advancements in medicine and our understanding of stem cells have led to a greater emphasis on further developing research focused on tissue engineering. This research has led to the rise of both two-dimensional and three-dimensional scaffolds that can be utilized to repair bone, skin, vascular, and potentially even nervous tissue. One of the prominent compounds used in modern scaffolds is collagen-based hydrogels due to their low antigenicity and ability to provide structure to cells. There is potential to further improve upon this three-dimensional scaffold by incorporating cellulose nanocrystals (CNCs) into a composite hydrogel with collagen. The addition would increase the mechanical strength of the composites compared to collagen alone. However, collagen and cellulose nanocrystals are both highly viscous and concentrated fluids for which improper mixing at inappropriate concentrations can lead to composites that contain aggregates of poorly dispersed collagen and cellulose nanocrystals. To prevent aggregation in the composites, several methods and protocols of mixing have been proposed and tested to create a protocol for homogenizing collagen and CNCs. In addition to this, compressive tests have been performed to determine the amount of mechanical strength that is added to these composites at varying concentrations of CNCs within the composite. The method that has resulted in the best homogenization is a 10-stepwise mixing approach. Using this method yielded a homogenous mixture that only has a 0.39% variance in rheological properties throughout the 10-step sample. It was shown that the Young's Modulus for collagen composites does not change significantly as CNC concentration increases, but the behavior of the hydrogels under stress changed from solely elastic to stress-softening followed by rapid strain-hardening with increasing CNC concentrations. Additionally, it was observed that increasing CNC concentration decreased porosity steadily, but the amount of porosity decrease may not be statistically significant. The porosity data cannot be used to make any conclusions though due to issues that arose during experimentation.

1 | INTRODUCTION

Tissue engineering is a growing field of study that heavily involves the use of biocompatible compounds and stem cells to create artificial matrixes that can sustain a population of cells to allow for better healing than what the body could do on its own. These scaffolds can and have been used for skin grafting, bone scaffolding, and vasculature, to name a few (Lee, Singla, & Lee, 2001). As the understanding of stem cells develops, the potential to repair tissues that previously were irreparable, such as nervous tissues, is becoming more realistically achievable (Lee et al., 2001). While there are several different types of scaffolds and scaffolding materials, a particularly interesting scaffold is a three-dimensional collagen scaffold that can be used to directly implant cells into tissues. The collagen scaffold has already been used in medical settings, and it has proven to be successful in procedures such as adipose tissue repair (León-Mancilla et al., 2021; Sawadkar et al., 2021). Collagen is chosen as the primary component of these scaffolds due to its various beneficial properties, which include but are not limited to high biocompatibility, biodegradability, bioabsorbability, synergy with bioactive components, non-antigenicity, and is compatible with synthetic polymers (Lee et al., 2001). This last quality is significant as it means that pure collagen scaffolds can benefit from the addition of polymers such as CNCs extracted from cellulose, which is the most abundant biopolymer on the planet (Sinah et al., 2015). CNCs have garnered interest due to their potential beneficial properties such as their low toxicity, biodegradability, and hydrophilicity (Samulin Erdem et al., 2019; Sinah et al., 2015). One interesting property of CNCs is their high mechanical strength, demonstrated by a

high Young's modulus value of 137 GPa. As it happens, the mechanical strength of collagen-based scaffolds is an area that can benefit from further improvement with the incorporation of CNCs (Sinah et al., 2015). CNCs also has been shown to be beneficial in biomedical applications, with studies showing that CNCs can expedite bone formation, encourage cell growth, promote vascularization, and have been used in biocomposites for rapid tissue and capillary regeneration (Sinah et al., 2015).

As collagen and CNCs both have biomedical applications, it seems reasonable to suggest that the two compounds would benefit from being in a composite with one another. Early studies have shown that CNCs provided beneficial properties such as mechanical strength to collagen scaffolds with no negative impact on cell growth (Li et al., 2014).

While the potential for collagen/CNCs scaffolds is apparent, the viability of these scaffolds depends on the quality of scaffolds that the mixture can be produced. An important aspect of any scaffold is homogeneity, or in other words, uniformity of a composite regardless of the location within the scaffold. In this sense, achieving homogeneity allows greater control of a scaffold's properties and composition at the cellular level. This is significant because cells incubated in environments that are not homogenous tend to proliferate in ways that are not homogenous as well, and this would bode poorly for scaffolds intended for medical use (Walsh & Malone, 1995).

This honors thesis's goal is to first determine if collagen and CNCs are chemically compatible and thus able to be mixed homogeneously. If possible, then it must be determined what is the best protocol for mixing collagen and CNCs to test for homogeneity. Once this is accomplished, testing was done to determine what method of mixing and molar concentration with our designed protocol leads to producing the most homogenous product. Following this, mechanical testing was done to test how the mechanical strength and porosity of scaffolds are impacted by varying concentrations of CNCs being added to homogenized composites. The results of this honors thesis will allow for the consistent fabrication of collagen and CNCs composites for future tissue engineering research purposes, and it will give additional insight into how CNCs alter the properties of collagen scaffolds.

1.1 | COMPREHENSIVE DISCUSSION OF COLLAGEN AND CNCs

Collagen is an organic molecule found in most portions of the human body. It is a critical component of bone, skin, vasculature, ligaments, tendons, muscles, the GI tract, and other systems in the body (Varma, Orgel, & Schieber, 2016). The reason for the multitude of applications for collagen is its ability to combine with molecules, which allows the function of collagen to be modified (Varma et al., 2016). While there are over 20 forms of collagen known, the form that is of interest in this project is collagen I. This form of collagen is the most abundant form in the body as it is a major component of the bones, skin, and internal organs. Collagen I is typically around 300nm long and is composed of three left-hand α helix chains that are approximately 1000 amino acids long (Varma et al., 2016). The chains twist to form the right-handed helix of the collagen molecule. The structure of collagen results in a molecular weight of about 300 kDa (Abraham, Zuenka, Perez-Ramirez, & Kaplan, 2008). Collagen, comprising of both hydrophobic and hydrophilic sidechains, demonstrates a hydrophilic nature making it soluble in water (Latorre, Lifschitz, & Purslow, 2016). This information indicates that collagen should be capable of being dissolved and mixed in an aqueous solution, a conclusion supported by work studying the ability of various solvents to dissolve collagen (Latorre et al., 2016).

A CNC particle, in general, is a crystalline portion of cellulose consisting of glucose rings that are connected by β -1,4 glycosidic linkage (Sinah et al., 2015). CNCs are produced via acid hydrolysis, which is followed by further breakdown utilizing the Nano DeBEE Homogenizer (Seo et al., 2018). While there are a variety of methods and acids that can be used to create CNCs, the acid used to form the CNCs in this study is sulfuric acid ($\text{H}_2\text{SO}_4^{2-}$). The use of sulfuric acid imparts a sulfate group onto the cellulose polymer during the reaction, and the homogenizer puts significant enough mechanical strain to separate the cellulose nanofibers from the nanocrystals. As a result of this process, CNCs contain hydroxyl and sulfate groups. These groups allow for extensive hydrogen bonding to occur, and as such the molecule exhibits hydrophilic properties (Sinah et al., 2015).

1.2 | DIAGNOSING ISSUES FACING HOMOGENIZATION

As was discussed above, both collagen and CNCs are molecules with hydrophilic natures that by all reason should be capable of mixing homogeneously in an aqueous solution of neutral pH. However, preliminary composite mixing resulted in CNC aggregates suspended within the collagen. Due to this observation, the physical properties of these compounds and the form in which they are utilized had to be taken into consideration. Both collagen and CNCs come in the form of highly viscous fluids. Viscous fluids, by their nature, require more force to shear and thus mix homogeneously. Considering this, it seems the issue of lack of homogeneity in the initial composites is not the result of incompatible compounds but instead an unoptimized mixing process.

Standard mixing practices have typically consisted of adding most or all the compounds to be mixed in a single step. While this method does work for many applications involving less viscous materials, it has been shown in many fields that viscous materials typically require a stepwise approach to mixing. The term stepwise here is used to describe the process by which a material is added to a solution in small portions, mixed thoroughly, and then repeated until the desired amount of material has been added. In the case of this project, stepwise mixing was tested against single-step mixing to determine if stepwise yields composites with a greater homogeneity. This will yield a protocol for mixing that consistently makes homogenous composite, which can then be used to test other properties of these composites.

1.3 | ALTERATION OF COLLAGEN SCAFFOLD PROPERTIES UPON ADDING CNCs

Collagen scaffolds are heavily researched within the biomaterials community and are already utilized in medical settings. These scaffolds form when collagen molecules undergo crosslinking, which is the process in which collagen molecules create chemical bonds with other collagen molecules to create networks of collagen fibers with space in between fibers that is suitable for cell growth. Current applications of collagen utilize the supportive and modifiable nature of collagen, which allows for collagen to be utilized in many different settings (Lee et al., 2001). However, there are still limitations to these scaffolds, one such being mechanical strength. It has been established that CNCs can impart mechanical strength to collagen scaffolds and that increased mechanical strength is a positive trait that would allow collagen to serve as the basis for more types of tissue repair (Sinah et al., 2015). This project specifically seeks to determine how Young's Modulus is impacted by the addition of CNCs, as this value is a measure of the compressive stiffness of a material. The next important question is how does the addition of CNCs affect other properties? The properties in question currently are the porosity and mechanical strength of the matrix. Porosity is the measure of the amount of air or void space

found within a compound. The porosity of a scaffold will directly impact its functionality, as it has an impact on cell nutrition, proliferation, migration, vascularization, and also allows native tissues to grow with the scaffold (Loh & Choong, 2013). Mechanical strength in this study is defined as the ability to resist compressive force, which is a useful property in scaffolds being used in more stressful environments such as bone matrix. CNCs being added to a collagen matrix will likely have an impact on both the mechanical strength and porosity of the scaffold, so it is the second objective of this thesis to determine the extent to which the mechanical strength and porosity of collagen/CNC scaffolds are impacted by varying concentrations of CNCs addition. Namely, it is expected that an increase in CNCs will increase mechanical strength at the expense of decreasing porosity.

2 | METHODS FOR SAMPLE PREPARATION

Samples for these experiments are prepared using a collagen solution with a concentration of 3.91 mg/mL. The CNCs used for making these samples are sulfonated CNCs that are prepared in-house and have a concentration of 10 mg/mL. To keep samples consistent, a target solids content concentration of 3 mg/mL total solids content was selected. This value has been shown in collagen-only scaffolds to be the optimal solids content to produce scaffolds by a partnering lab in this project. Also, keeping a solids content ensures that when tests for homogeneity, mechanical strength, and porosity are conducted, the only variable to consider is the varying concentrations of collagen and CNC within a sample. All samples were mixed by hand with a hand spatula in a microcentrifuge tube. This method was chosen as this serves as the current standard practice in other studies concerning collagen/CNC scaffolds.

Sample concentrations were determined by dictating the mass quantity CNC was contributing to the final solids content of 3 mg within 1 mL of solution. For example, a 10% CNC mixture would have 0.3 mg of CNC and 2.7 mg of collagen, which would equate to 30 μ L of CNC solution and 690.54 μ L of collagen solution. However, the volume of either solution needed to achieve the proper mass of solids content is not sufficient to create a single milliliter of fluid. To get the proper volume of one milliliter, 10 μ L of Calcofluor White (CW) and 269.46 μ L of deionized water were added. The water and CNCs are combined before adding to the solution, to make the addition of CNCs into the solution easier when it is diluted into a larger volume before mixing. This adds up to 1000 μ L of volume while still having 3 mg/mL of solids content. CW is a fluorescent dye whose use will be discussed in a later section. There will also be a stepwise component to mixing. The CNC/water mixture was added in a predetermined number of steps, and the volume added per step was calculated by dividing the volume CNC/water mixture by the amount of desired mixing steps. In between each addition of CNC/water, mixing will occur for one minute. CW is added at the end of all mixing, and the sample is then allowed to rest for 2 minutes so that CW may bond to the CNCs.

The full procedure for mixing a composite using a 10% CNCs concentration in 10 steps as an example is as follows. First, collagen (2.7 mg or 690.54 μ L of solution) is added to a microcentrifuge tube. A volume of 30 μ L of CNC solution is added to 269.46 μ L of deionized water. Following this, a volume of 29.94 μ L of CNC/water mixture was added to the collagen and then mixed for 1 minute. This process would be repeated 9 additional times, which would allow for the full volume of CNC/water mixture to be added to the collagen. Following the 10th addition of the CNC/water mixture, the CW would be added and mixed into the solution for 1 minute and then allowed to rest for 2 minutes.

2.1 | HOMOGENEITY TESTING

Homogeneity testing will comprise of a preliminary imaging test and then followed by rheology testing. The imaging test was used to quickly determine what number of steps in stepwise mixing seems to produce results that encourage homogenous mixing. This is done by imaging the fluorescent properties of CW while under ultraviolet light in a controlled setting. The setting where mixing and imaging was done was in a cold storage room, as this prevented premature hydrogel formation. CW is a dye that binds nonspecifically to the β -1,4 glycosidic linkages in CNCs. Collagen has no such bonds and thus CW will not bind to it. Once bound to CNCs, CW will fluoresce in ultraviolet light. Since CW will bind to CNCs and not collagen, aggregation of CW-bound CNC is readily apparent when held under UV light.

The imaging test will consist of multiple tests that test the effectiveness of adding increasing numbers of partitions to the mixing process. The number of steps tested was 1, 2, 5, 10, and 15. The single-step mixing serves as the experimental control as this is the standard mixing procedure before this experiment. Samples were all tested at 10% CNCs concentration. 10% CNCs concentration was the highest concentration of CNCs that were tested for mechanical strength and porosity, so if homogeneity can be proven it would be valid to assume that lower concentrations of CNCs are homogenous as well. Each sample was imaged while in the microcentrifuge tube in the upright (vertical) and sideways (horizontal) positions for which multiple images of each sample were taken. Images were then analyzed for signs of homogeneity. This was done by looking at images and looking at the size of aggregated particles and solution fluorescence. A sample with increased homogeneity would be expected to have finer aggregate and brighter solution fluorescence. Solution fluorescence indicates homogeneity as CNCs that are too small to see are what causes the solution to appear brighter. Thus, the brighter the solution, the more finely distributed CNCs there are in the solution. Image analysis will also be done by recording the RGB values of 10 pixels that are randomly selected from the portion of the images that depict the composite solution. RGB values indicate the amount of red, green, and blue used to create the color that is seen in each pixel. A value of 0 means none of that color is present, and a value of 255 means that the maximum amount of that color is present in the pixel. This also means that a value of 0 in all colors makes a pixel black, and a value of 255 in all values makes the pixel white. These properties allow for the determination of color “brightness” by keeping two RGB values constant and allowing a third to vary. For all test samples, the red value is at or near zero and the blue value is at its maximum value of 255. Due to these values being constant, the green value can be used as a quantitative measure of solution brightness, and as stated before, a greater solution fluorescence is attributed to a higher degree of homogeneity. The dependent variable in RGB testing for homogeneity was the green value in pixels sampled from the protocol images. A t-test was also performed to determine if the amount of homogeneity indicated by the mean values for green was significantly different. The three protocols that were indicated to be the most homogenous by these tests were then further studied using rheological testing.

Rheology testing was conducted using the Discovery HR 2 Hybrid Rheometer (DHR2) from TA Instruments, New Castle, Delaware. The samples tested will comprise those shown to have increased homogeneity from the imaging test, and each sample type was tested 3 times. Utilizing the DHR2’s software, preliminary samples were tested to determine the model that best fits the rheological properties. The tests yielded that the Carreau model was the best fit for the data

which graphed viscosity versus shear rate. The equation associated with this model is listed below.

$$\mu_{eff}(\gamma) = \mu_{inf} + (\mu_o - \mu_{inf})(1 + (\lambda\gamma)^2)^{\frac{n-1}{2}}$$

In this model, μ_{eff} is viscosity dependent on shear rate, γ . The variable μ_{inf} is the viscosity at infinite shear rate, λ is the characteristic time in seconds, and n is the power index. The variable μ_o is the initial rate viscosity with a unit of Pa•s. The initial rate viscosity is found using this model within the DHR2's software twice per sample. The first initial rate viscosity corresponds to one-half (500 μ L) of each sample, and the second initial rate viscosity corresponds to the other half of a sample. Based on previous studies, these two measurements should have less than a 10% difference in viscosity if homogenous (Dani et al., 2021). The difference in viscosity within a sample is calculated as follows.

$$\% \text{ Difference} = \frac{\mu_{o,2} - \mu_{o,1}}{\mu_{o,2}} \times 100$$

Once all the samples have been tested, the data was analyzed to determine which number of steps can yield a homogenous mixture with the fewest number of mixing steps. This was done by collecting μ_o for every sample twice. All the first 500 μ L measurements were averaged together, and all second 500 μ L measurements were averaged together. Once averaged, the first sample initial rate viscosities and the second sample initial rate viscosities were used to calculate the percent difference of the initial rate viscosities found in each data set. A paired two-sample t-test was performed to determine if the difference between the means of the first test and second test of samples is statistically significant. This test was chosen as the data for rheology testing was gathered in pairs for each sample, and this test accounts for data collected in pairs under homogenous conditions. A test of this nature allowed for the determination that the homogeneity achieved for each protocol was statistically significant. The statistical t-test was performed with a significant value (α) of 0.05. The null hypothesis for this test was that the difference between the mean values of the first and second tests for initial rate viscosity is zero. The T-value for this test is calculated with the below equation.

$$T = \frac{D - \Delta_o}{\sigma/\sqrt{n}}$$

In this equation, D is the sample average of the n differences. The variable Δ_o represents the null hypothesis value of the difference between the two data sets' means, which is zero in this case. The value σ represents the standard deviation and n represents the number of pairs observed. A t-test was performed between the different protocols as well to determine if there was a significant difference in the amount of homogeneity produced by different protocols. For this test, the parameter of interest is the mean percent difference produced by different protocols. The t-test between protocols was chosen to determine if the difference in homogeneity between protocols was significant. If there were protocols that were similar in homogeneity, then the results of RGB testing were used to determine the best protocol.

2.2 | MECHANICAL STRENGTH AND POROSITY TESTING

Testing the mechanical strength and porosity of the collagen/CNC composites was done by altering the concentration of CNCs within the composite and curing the composite into a hydrogel form. The concentrations tested were 0, 2.5, 5, 7.5, and 10% CNCs by mass. The method for calculating the amount of CNCs in each sample is the same as was described in the homogeneity testing. All samples will also be mixed utilizing a 10-step method, because of the verification that this method yielded a homogeneous mixture utilizing the fewest number of steps.

Two major key differences in sample preparation are that Sodium Hydroxide (NaOH) and Phosphate Buffered Saline (PBS) were added to the solution in place of deionized water. The collagen and CNCs solutions used in this project are slightly acidic, and for collagen crosslinking to occur, a neutral to very slightly basic pH is required (~7.4 pH). This necessitates the addition of NaOH to achieve a proper pH. PBS is a solution that mimics the ECM and is commonly used to create biological systems. PBS contains NaCl, KCl, Na₂HPO₄, and KH₂PO₄. These salts are necessary to encourage cross-linking, and the solution is a nonreactive buffer with a pH of 7.4. Upon making a sample, it was cured for 1.5 hours at 37.0°C to allow crosslinking to occur within the collagen matrix. This amount of time also allows excess water to evaporate, making the hydrogels easier to handle. Upon making samples, some were used for compressive mechanical strength testing, and others were used to test for porosity.

The gels were tested in their hydrated form to assess the mechanical strength of wet samples, which is more relevant to the future studies of this research work. Cured hydrogels of each concentration were placed in the DHR2 where compression testing will take place. Compression testing consists of placing the cured hydrogels on the testing pedestal of the DHR2. Once the hydrogel is placed, the DHR2's head begins to compress the hydrogel. The DHR2 will induce increasing amounts of strain to the bead and will monitor the amount of stress required to induce that amount of strain. The test ends when 100% strain is induced. At this point, the hydrogel has been completely crushed. The DHR2's software will export the data into a tabularized and graphical form which will then be used for data analysis. The Young's Modulus was found for multiple samples of each concentration. Young's Modulus, also called the modulus of elasticity, is related to stress and strain according to the equation below.

$$Y = \frac{\sigma}{\epsilon}$$

In the equation, σ represents stress and ϵ represents strain. Data collected from the DHR2 was used to make a stress versus strain plot, and the Young's Modulus of the tested material is given as the slope of the linear portion of growth in the plot. This value was found in the data exported by the DHR2 by performing multiple linear regressions and then selecting the data in which the highest coefficient of determination (R^2) value. To ensure that the results are not skewed, the value for Young's Modulus will only come from samples of data that contain segments of 10% strain or more. This will decrease the R^2 value associated with values found in this manner, but it will also prevent the need to selectively choose data points. Once Young's Modulus is measured for all samples, a mean Young's Modulus value for each concentration was calculated to allow for comparison between concentrations. The stress on the samples will also be notated at the strains of 60%, 70%, 80%, and 90% as another form of comparison between samples of different concentrations. A t-test was also performed to determine if the difference in the mean Young's Modulus values were significantly different.

Porosity testing was conducted using freeze-dried samples. Freeze drying begins with first freezing the samples until they reach a temperature of -80°C . Once frozen, the samples are loaded into a freezing vessel and attached to the freeze drier. The freeze drier then creates a vacuum and begins to maintain a temperature of -50°C . The vacuum and frigid temperatures cause the water within the sample to undergo sublimation. This removes the water while still maintaining the internal structure of the hydrogel, which makes it possible to test the amount of space within the hydrogel during rehydration. After the 36-hour freeze-drying process, the mass of every sample was taken to serve as a measurement for the samples when all mass is due to the collagen/CNC structure. Following freeze-drying and initial weighing, the freeze-dried samples were placed in water for 6 hours. It is assumed that after 6 hours, the samples are once again hydrated fully and are not capable of holding any more mass in terms of water. After 6 hours, the mass of the hydrogels was taken again. These two values will allow the calculation of porosity using the below equation.

$$\text{Porosity} = \frac{\frac{(W_2 - W_1)}{\rho_{H_2O}}}{\frac{W_1}{\rho_b} + \frac{(W_2 - W_1)}{\rho_{H_2O}}}$$

The value W_2 is the post-soaking mass of the fully hydrated scaffolds, W_1 is the pre-soaking mass of the scaffolds when fully dehydrated, ρ_{H_2O} is the density of water, and ρ_b is the bulk density of collagen/CNC solution. The bulk density is the density of a substance including the space between and within particles. The bulk density represents the dependent variable with this test, as it is directly impacted by the amount of CNC and collagen in the tested samples. The bulk density of the solution is calculated using the equation below.

$$\rho_b = (\% \text{ CNC})\rho_{\text{CNC}} + (1 - \% \text{ CNC})\rho_{\text{Collagen}}$$

The bulk density of the CNCs solution used in the experiment was 1.54 g/cm^3 . This value was provided by the lab where this thesis was conducted. The bulk density of collagen is 1.42 g/cm^3 (Morin, Hellmich, & Henits, 2013). Using the formula above and the concentrations of CNCs chosen for experimentation, the bulk densities of the solution to be tested are listed in the table below.

Table 1: Bulk densities to be used in porosity calculations.

CNC Concentration (%)	Bulk Density (g/cm^3)
0.0%	1.42
2.5%	1.423
5.0%	1.426
7.5%	1.429
10.0%	1.432

3.1 | HOMOGENEITY TESTING RESULTS AND ANALYSIS

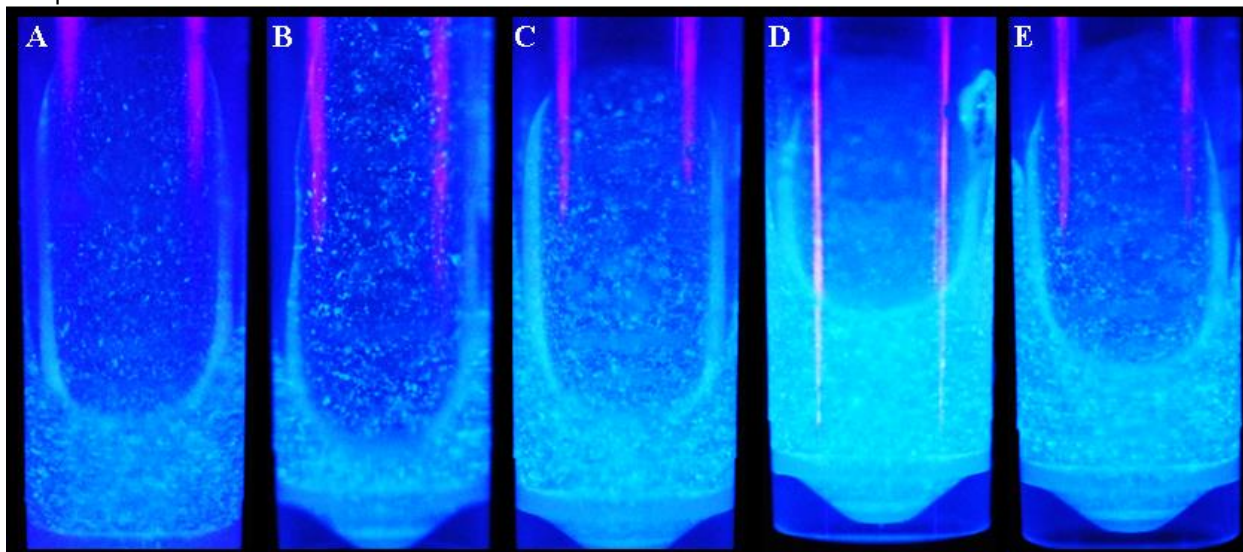


Figure 1: The above image depicts the results from image testing. The samples pictured are as follows: A-1 Step Mixing, B-2 Step Mixing, C-5 Step Mixing, D-10 Step Mixing, E-15 Step Mixing

The images above are the results of 1, 2, 5, 10, and 15-step mixing. The degree of mixing increases with an increasing number of stepwise additions from left to right, and when looking at the photographs, both the size of aggregate particles and the fluorescence of the total solution must be considered. The first two samples have little to no fluorescence in the general solution, and the aggregates are large and visible. These results led to the conclusion that 1-step and 2-step mixing are not homogenous. The next two samples of note were the 5-step and 15-step mixing. The images now display aggregates still, but solution fluorescence is now visible. The 10-step mixing sample shows the most promising results based purely on imaging. It has fine aggregate particles, and the solution fluoresces the brightest out of all samples. The RGB results of imaging are displayed below and provide additional insight into the homogeneity of the mixtures pictured in Figure 1.

Table 2: Average RGB values for each sample

Sample	R-Value	G-Value	B-Value
1-Step	0.9	145	255
2-Step	0	165.4	255
5-Step	0	193.6	255
10-Step	0.1	221.4	255
15-Step	0	194.7	255

Table 2 indicates that the three brightest results in decreasing order were 10-step, 15-step, and 5-step mixing. This was confirmed by the t-test, which indicated that 10-step, 15-step, and 5-step mixing were significantly more homogenous than 1-step and 2-step. 10-step was also shown to be significantly more homogenous than the 5-step and 15-step mixing protocols. Based on these results, the first mixing method to be selected for rheology mixing was the 10-step mixing, as it

exhibits qualities that appear to be the result of homogeneity. Mixing types 15-step and 5-step mixing were also chosen for further testing as they exhibited homogenous qualities during imaging as well. The results of rheology testing on these mixing types are depicted below.

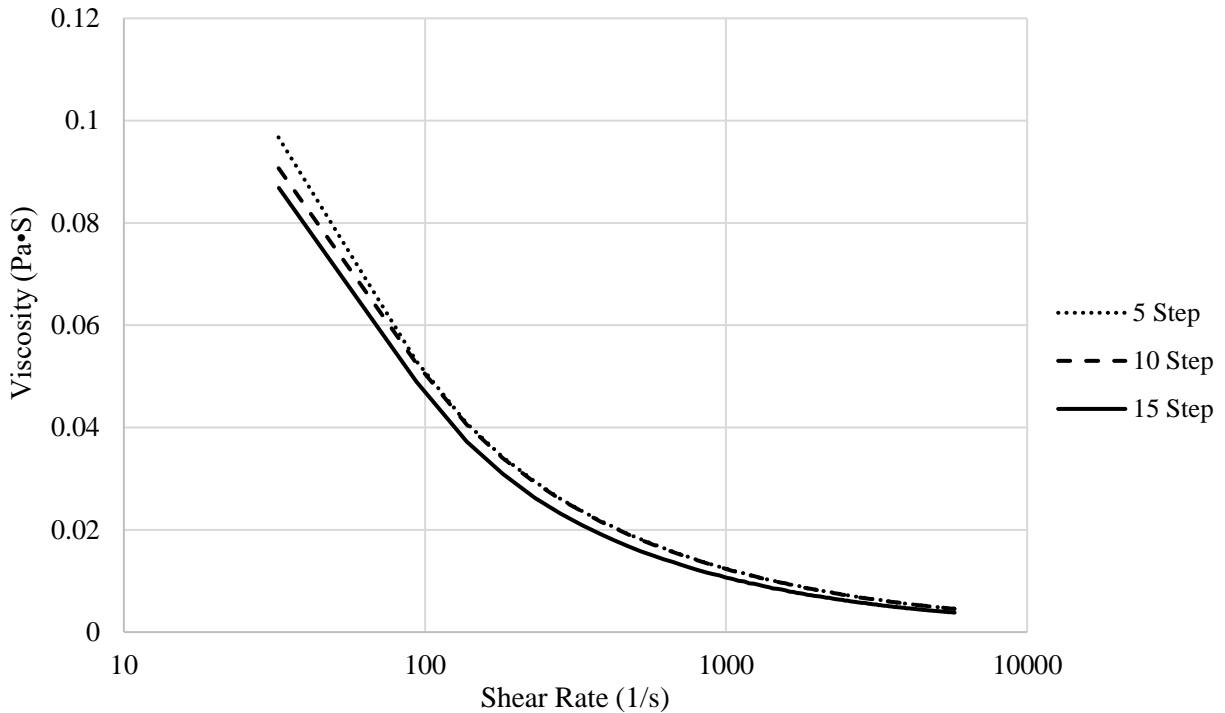


Figure 2: Viscosity versus the shear rate at varied stepwise mixing processes.

The graph above includes the viscosity results for all three mixing types promoted to rheological testing following confirmation of homogeneity via imaging analysis. Interestingly, as the number of mixing steps increases, the viscosity of the solution seems to decrease despite having the same composition. This trend persists with an increasing shear rate as well. More significantly, the data gathered allowed for the initial rate viscosities to be determined for all samples for comparison. The results of the data analysis are depicted below. To see a table of all the initial rate viscosities measured and the T-test results, see Table 3 in the appendix.

Table 3: Results of Rheology Testing

Sample Type	Round 1 mean μ_o (Pa·s)	Round 2 mean μ_o (Pa·s)	% Difference	T-score	P-Value
5-step	0.2068	0.1504	27.27%	0.804	0.506
10-step	0.1500	0.1506	0.39%	-0.039	0.972
15-step	0.1538	0.1528	0.63%	0.051	0.964

The results of the rheology testing provide further confirmation of the apparent homogeneity that was detected in the imaging testing for 5, 10, and 15-step mixing. The t-test determined that there was no statistically significant difference between the means of the initial rate viscosities of the first and second tests for any of the stepwise protocols. This further indicates that these

protocols created composites that have increased homogeneity. The t-test to compare the mean % difference between protocols determined that there was no significant difference between homogeneity produced by different protocols. Due to this, the results of RGB testing were used to determine which protocol would be used for testing going forward, and since 10-step mixing was the most homogeneous in RGB testing, it was selected as the best mixing protocol.

3.2 | MECHANICAL STRENGTH AND POROSITY RESULTS AND ANALYSIS

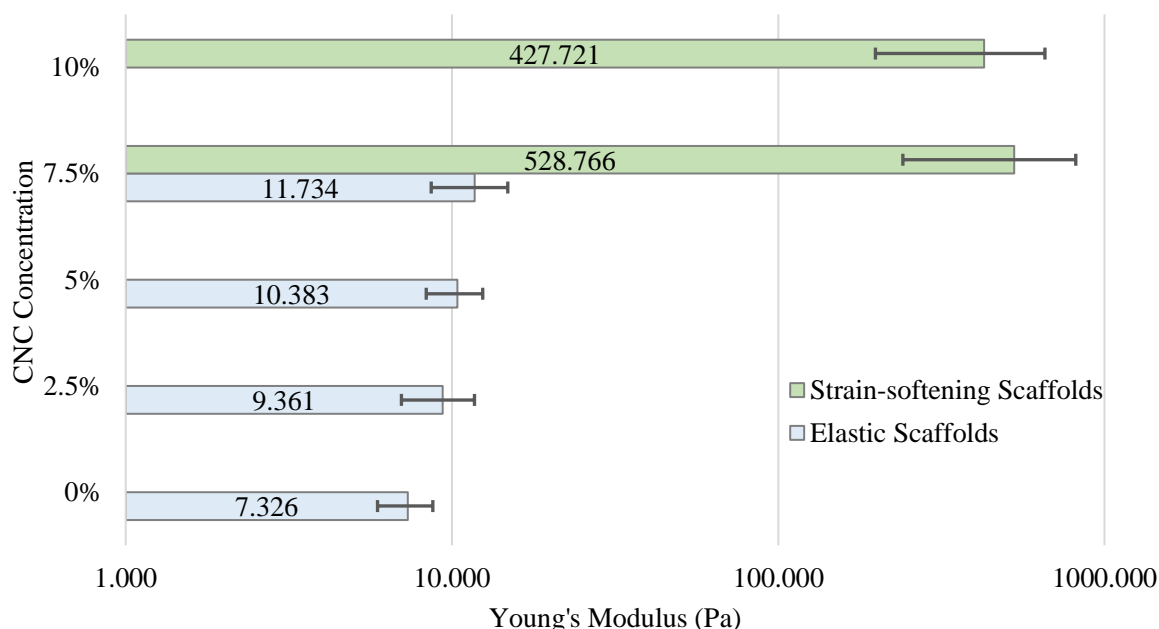


Figure 4: Semi-log plot for Young's modulus values at varied CNC concentrations.

The results of the mechanical strength testing appeared to demonstrate there was no significant increase in strength when analyzing the Young's Modulus for various concentrations, but it is also clear that the way the composite behaves when under stress changes with increasing concentrations of CNCs within samples increases. At lower concentrations, the composite behaves elastically. As the strain experienced by the hydrogel increases, the stress required to achieve that strain increases as well. As the concentration of CNCs increases though, namely once it reaches 7.5% in this study, the gel composites withstand more stress but also exhibit strain softening. Then after sufficient pressure, rapid strain hardening is shown. This behavior is the reason for the drastic change in Young's Modulus that is seen, as the only time that the hydrogel resists deformation is when nearing 80-90% strain, after which the amount of stress required to induce further strain begins to increase dramatically. An example of this phenomenon where a 0% CNC and 10% CNC sample are having their behaviors compared can be found in Figure 10 in the appendix. Because subsets of the 7.5% samples behave either elastically or with strain-softening properties, the Young's Modulus data for the 7.5% CNCs concentration initially had a large standard deviation, which is why the graph above separated scaffolds in the study based on CNC concentration and behavior type. To provide insight into scaffolds that exhibit similar behavior, graphs that depict the 7.5% CNC's Young's Modulus for elastic and strain softening samples separately are found in Figure 6 and Figure 7 in the appendix. These

occurrences indicate that the mechanical properties of collagen composites with high concentrations of CNCs need to be further studied. To better understand the data, it is also appropriate to analyze the amount of stress on the composites at various strains. This data is graphed below.

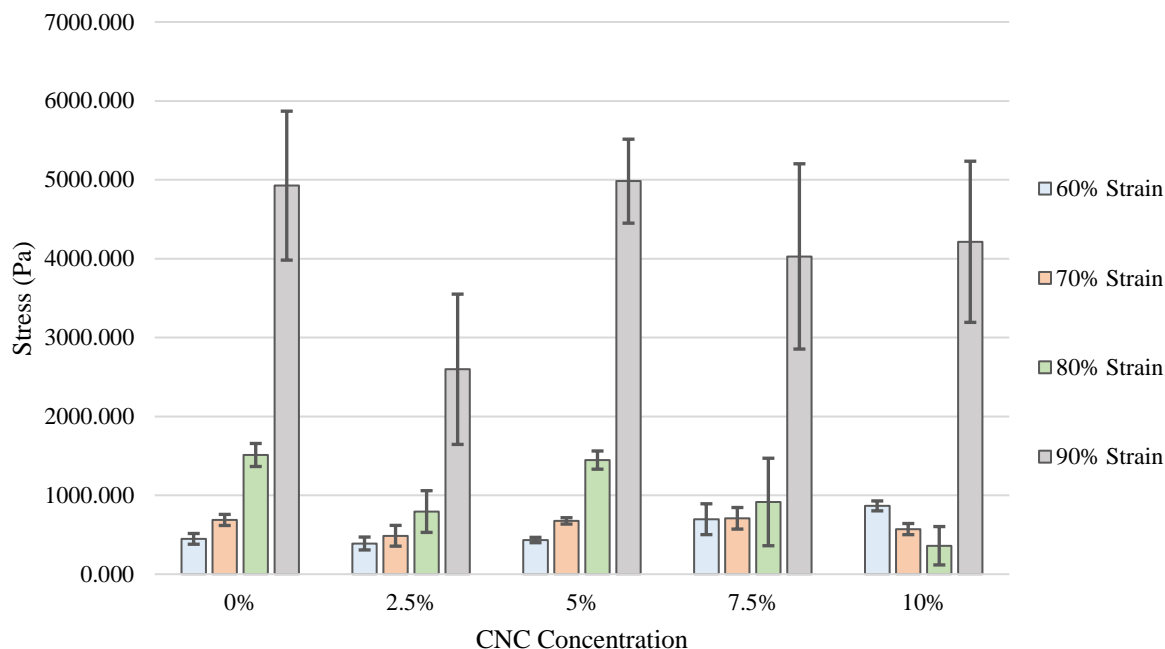


Figure 5: *Depicts the mean stress placed on different concentrations of composite gels at various strains.*

This data suggests that the 0%, 2.5%, 5%, and 7.5% concentrations have a correlation between stress and strain, though, once again, some 7.5% samples exhibited strain softening. The 10% CNCs concentration sample exhibited shear softening and rapid strain hardening in all the samples. The amount of stress at lower strains was also higher for compounds of higher CNCs concentrations, which can be seen when comparing the 10% samples to the collagen-only (0%) samples. As with the Young's Modulus results, graphs depicting the mean stress on various strains for elastic scaffolds and strain softening scaffolds separately are found in the appendix as Figure 8 and Figure 9. Following mechanical testing, the porosity of the hydrogels was determined. The findings for mechanical strength testing were ultimately unexpected, and possible reasons for these findings will be discussed in the conclusion. The results of porosity testing are displayed below.

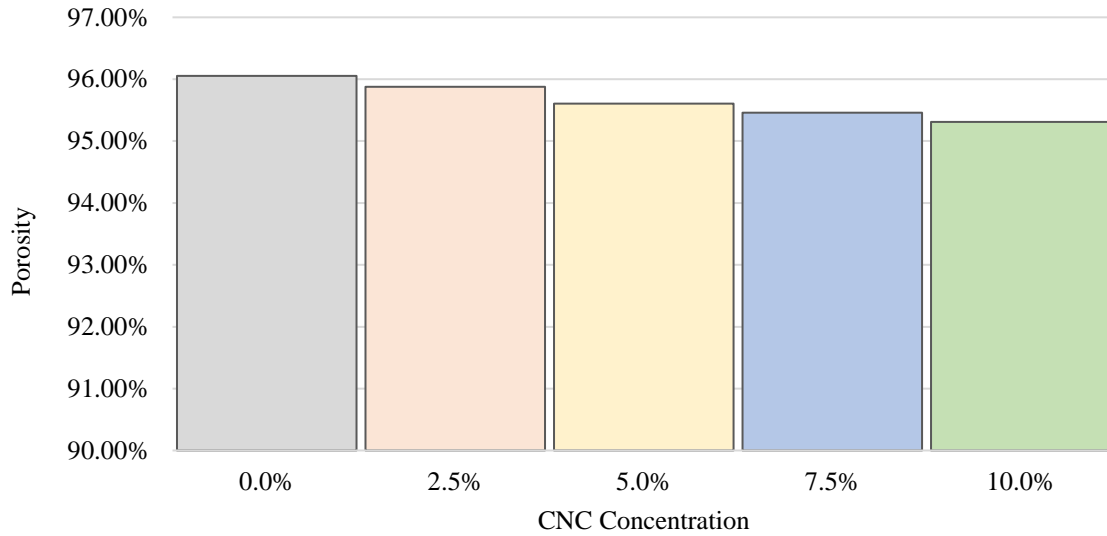


Figure 3: Porosity test using different concentrations of CNC in a 10-stepwise approach.

Table 4: Porosity data and statistical analysis

Sample	W1 (g)	W2 (g)	Porosity
0.0%	0.0036	0.0653	96.05%
2.5%	0.0035	0.0607	95.88%
5.0%	0.0047	0.0764	95.61%
7.5%	0.0031	0.0487	95.46%
10.0%	0.0042	0.0638	95.31%

During the porosity testing, technical difficulties only made it possible to run a single trial for porosity testing. The freeze-dried samples were so light that all samples had to be used in a single test to obtain any data. As such, the results collected were used as an indicator of what the data may be suggesting, but no definitive conclusions can be drawn from the data. The results indicate that there is a slight decrease in porosity as CNC concentration increases, but it is impossible to tell if this decrease is significant since there was only one observation in this trial. It was hypothesized that increasing the concentration of CNCs would decrease porosity, and while that seems to be occurring, a concentration of 10% CNCs only decreased porosity by about 0.7% from the 0% CNCs concentration. This is not a large decrease in porosity, and it is possible that this finding would not be statistically significant if more data was collected. Due to the possibility that CNCs may not have a substantial impact on porosity, further research should be done to confirm this result.

4 | DISCUSSION AND CONCLUSION

The results of homogeneity testing via imaging and rheology testing conclude that the minimal amount of mixing required to make a homogenous mixture is mixing in 10 steps with 1 minute of mixing in each step. It was shown that there was a 0.39% variation in rheological properties within the 10-step samples, which has been proven in other studies to indicate homogeneity. If further improvement of the collagen and CNCs mixture homogenization were to be studied in the future, more intense mixing methods could be tested, as only hand mixing was tested in this project. Compressive mechanical strength testing indicated that as CNC concentration increased,

the Young's Modulus did not change significantly for scaffolds that exhibited similar behaviors. The mechanical strength test also indicates that samples with higher CNCs concentrations in collagen began to exhibit different strain behavior, as shown by the initial strain softening followed by strain hardening. The lack of change in mechanical strength was not an expected result. The first possibility for a lack of change in mechanical strength could be that composite homogeneity was lost during the curing process, which would not allow the CNCs to impart their strength properly to the scaffolds. This suggestion arises from imaging that was performed on scaffolds following the curing process. This image is found below.

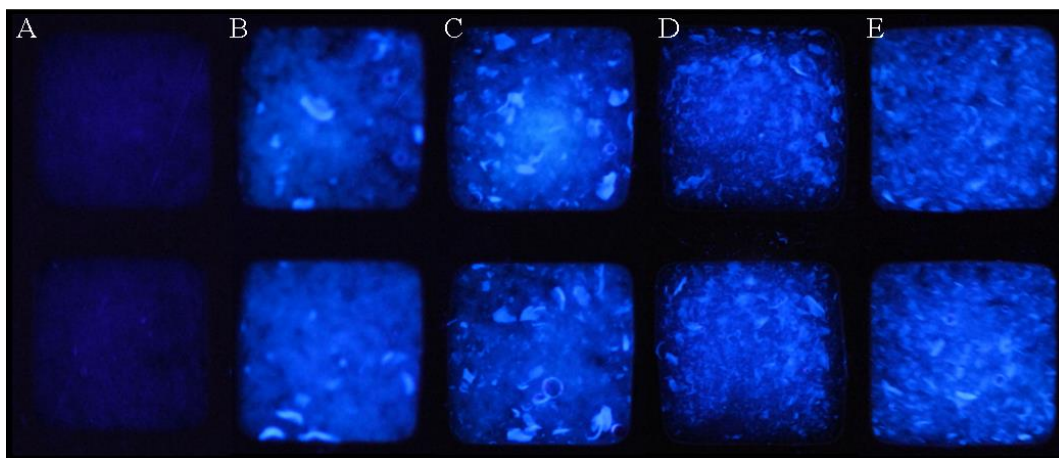


Figure 4: UV imaging of scaffolds. The CNCs concentration for the different scaffolds are A-0%, B-2.5%, C-5%, D-7.5%, E-10%

As can be seen in the images, some aggregates formed during the curing process were not present while the gel was still a solution. This could indicate that the homogeneity of the scaffolds was lost during the curing process somehow. Another possible explanation for no significant change in mechanical strength could be that the data collection and analysis were not powerful enough to detect a change. The mean Young's Modulus was steadily increasing, so it is plausible that if more data was collected or a more powerful test statistic was selected, the change in strength would be statistically significant. It is suggested that future research be conducted on determining how homogenous cured hydrogels are, and it is believed it would be beneficial to test multiple aspects of the scaffolds to better understand scaffold strength. Possible test statistics could include tensile strength or resistance to shear forces. The behavior change, while unexpected, may simply be a product of increasing CNC concentration. The fact that some 7.5% samples and all 10% samples exhibited strain-softening behavior seems to indicate that CNCs impart enough properties to scaffolds at these concentrations to alter overall scaffold behavior. It is recommended that testing be done to determine the CNC concentration at which behavior changes. Following this, it would be beneficial to study the properties of scaffolds that behave elastically and those that exhibit strain-softening behavior separately.

Porosity testing cannot be used to draw any definitive conclusions as there was not enough data collected, but the results that were collected do encourage further study as they seem to indicate that there is no statistically significant change in porosity. In summation, the project succeeded in producing homogenous samples utilizing a 10-step, step-wise mixing process. It was also determined that CNCs had no significant impact on strength but did change scaffold behavior, and more testing must be done to determine how CNC concentration affects porosity.

REFERENCES

- Abraham, L. C., Zuenen, E., Perez-Ramirez, B., & Kaplan, D. L. (2008). Guide to collagen characterization for biomaterial studies. *Journal of Biomedical Materials Research. Part B, Applied Biomaterials*, 87(1), 264–285. <https://doi.org/10.1002/jbm.b.31078>
- Dani, S., Ahlfeld, T., Albrecht, F., Duin, S., Kluger, P., Lode, A., & Gelinsky, M. (2021). Homogeneous and Reproducible Mixing of Highly Viscous Biomaterial Inks and Cell Suspensions to Create Bioinks. *Gels (Basel, Switzerland)*, 7(4), 227. <https://doi.org/10.3390/gels7040227>
- Latorre, M. E., Lifschitz, A. L., & Purslow, P. P. (2016). New recommendations for measuring collagen solubility. *Meat Science*, 118, 78–81. <https://doi.org/10.1016/j.meatsci.2016.03.019>
- Lee, C. H., Singla, A., & Lee, Y. (2001). Biomedical applications of collagen. *International Journal of Pharmaceutics*, 221(1–2), 1–22. [https://doi.org/10.1016/s0378-5173\(01\)00691-3](https://doi.org/10.1016/s0378-5173(01)00691-3)
- León-Mancilla, B., Martínez-Castillo, M., Medina-Avila, Z., Pérez-Torres, A., Garcia-Loya, J., Alfaro-Cruz, A., ... Gutierrez-Reyes, G. (2021). Three-Dimensional Collagen Matrix Scaffold Implantation as a Liver Regeneration Strategy. *Journal of Visualized Experiments: JoVE*, (172). <https://doi.org/10.3791/62697>
- Li, W., Guo, R., Lan, Y., Zhang, Y., Xue, W., & Zhang, Y. (2014). Preparation and properties of cellulose nanocrystals reinforced collagen composite films. *Journal of Biomedical Materials Research. Part A*, 102(4), 1131–1139. <https://doi.org/10.1002/jbm.a.34792>
- Loh, Q. L., & Choong, C. (2013). Three-Dimensional Scaffolds for Tissue Engineering Applications: Role of Porosity and Pore Size. *Tissue Engineering. Part B, Reviews*, 19(6), 485–502. <https://doi.org/10.1089/ten.teb.2012.0437>

- Morin, C., Hellmich, C., & Henits, P. (2013). Fibrillar structure and elasticity of hydrating collagen: A quantitative multiscale approach. *Journal of Theoretical Biology*, 317, 384–393. <https://doi.org/10.1016/j.jtbi.2012.09.026>
- Samulin Erdem, J., Alswady-Hoff, M., Ervik, T. K., Skare, Ø., Ellingsen, D. G., & Zienolddiny, S. (2019). Cellulose nanocrystals modulate alveolar macrophage phenotype and phagocytic function. *Biomaterials*, 203, 31–42. <https://doi.org/10.1016/j.biomaterials.2019.02.025>
- Sawadkar, P., Mandakhbayar, N., Patel, K. D., Buitrago, J. O., Kim, T. H., Rajasekar, P., ... Gareta, E. G.-. (2021). Three dimensional porous scaffolds derived from collagen, elastin and fibrin proteins orchestrate adipose tissue regeneration. *Journal of Tissue Engineering*, 12, undefined-undefined. <https://doi.org/10.1177/20417314211019238>
- Seo, Y.-R., Kim, J.-W., Hoon, S., Kim, J., Chung, J. H., & Lim, K.-T. (2018). Cellulose-based Nanocrystals: Sources and Applications via Agricultural Byproducts. *Journal of Biosystems Engineering*, 43(1), 59–71. <https://doi.org/10.5307/JBE.2018.43.1.059>
- Sinah, A., Martin, E. M., Lim, K.-T., Carrier, D. J., Han, H., Zharov, V. P., & Kim, J.-W. (2015). Cellulose Nanocrystals as Advanced “Green” Materials for Biological and Biomedical Engineering. *Journal of Biosystems Engineering*, 40(4), 373–393. <https://doi.org/10.5307/JBE.2015.40.4.373>
- Varma, S., Orgel, J. P. R. O., & Schieber, J. D. (2016). Nanomechanics of Type I Collagen. *Biophysical Journal*, 111(1), 50–56. <https://doi.org/10.1016/j.bpj.2016.05.038>
- Walsh, P. K., & Malone, D. M. (1995). Cell growth patterns in immobilization matrices. *Biotechnology Advances*, 13(1), 13–43. [https://doi.org/10.1016/0734-9750\(94\)00021-4](https://doi.org/10.1016/0734-9750(94)00021-4)

APPENDIX

Table 5: Displays the initial rate viscosity data taken during rheology testing.

Sample	Round 1 μ_o (Pa•s)	Round 2 μ_o (Pa•s)	Difference	% Difference
5 step, 1	0.151009	0.183462	0.032453	17.69%
5 step, 2	0.172965	0.166148	0.006817	3.94%
5 step, 3	0.296445	0.101595	0.194850	65.73%
St. Dev	0.078402	0.043145	0.101969	32.44%
10 step, 1	0.148184	0.159822	0.011638	7.28%
10 step, 2	0.106105	0.125092	0.018987	15.18%
10 step, 3	0.195657	0.166775	0.028882	14.76%
St. Dev	0.044803	0.022331	0.008653	4.44%
15 step, 1	0.165485	0.152313	0.013172	7.96%
15 step, 2	0.146455	0.120412	0.026043	17.78%
15 step, 3	0.149438	0.185724	0.036287	19.54%
St. Dev	0.010235	0.032659	0.011582	6.24%

Table 6: RGB Values for Randomly Selected Pixels

	1-step			2-step			5-step			10-step			15-step		
	R	G	B	R	G	B	R	G	B	R	G	B	R	G	B
1	0	140	255	0	144	255	0	218	255	1	234	255	0	191	255
2	0	143	255	0	189	255	0	177	255	0	218	255	0	189	255
3	0	142	255	0	156	255	0	206	255	0	221	255	0	210	255
4	4	151	255	0	152	255	0	204	255	0	230	255	0	197	255
5	0	163	255	0	181	255	0	199	255	0	230	255	0	224	255
6	0	151	255	0	145	255	0	182	255	0	215	255	0	186	255
7	1	132	255	0	188	255	0	176	255	0	225	255	0	192	255
8	4	153	255	0	168	255	0	178	255	0	221	255	0	200	255
9	0	136	255	0	160	255	0	206	255	0	201	255	0	176	255
10	0	139	255	0	171	255	0	190	255	0	219	255	0	182	255
Average	0.9	145	255	0	165.4	255	0	193.6	255	0.1	221.4	255	0	194.7	255
	St. Dev	9.333		St. Dev	16.734		St. Dev	14.968		St. Dev	9.395		St. Dev	14.008	

5%			t-Test: Paired Two Sample for Means		
sample	test1	test2			
1	0.151009	0.183462			
2	0.172965	0.166148			
3	0.296445	0.101595			
Mean				0.206806333	0.150401667
Variance				0.006146834	0.001861512
Observations				3	3
Pearson Correlation				-0.998107309	
Hypothesized Mean Difference				0	
df				2	
t Stat				0.80411793	
P(T<=t) one-tail				0.25285881	
t Critical one-tail				2.91998558	
P(T<=t) two-tail				0.50571762	
t Critical two-tail				4.30265273	

Figure 5: Paired T-test results

Table 7: Mechanical Strength Testing Data for all CNC concentrations

0%						
Sample	Young's Modulus (Pa)	R ²	60% stress	70% stress	80% stress	90% stress
1	6.721	0.980	370.123	621.426	1384.310	4388.400
2	5.994	0.989	457.039	690.617	1631.070	6086.780
3	6.360	0.981	554.786	803.158	1670.930	5808.240
4	9.362	0.979	439.053	679.884	1527.850	4259.440
5	8.191	0.935	417.197	642.210	1340.800	4084.630
Average	7.326		447.640	687.459	1510.992	4925.498
2.5%						
Sample	Young's Modulus (Pa)	R ²	60% Stress	70% modulus	80% modulus	90% modulus
1	8.108	0.944	324.630	352.007	471.598	1141.200
2	7.267	0.926	322.816	411.527	784.087	2692.560
3	14.669	0.939	359.581	440.394	751.096	2356.150
4	9.991	0.951	336.680	408.694	598.622	1934.940
5	8.049	0.965	352.984	420.014	638.450	2467.500
6	8.064	0.961	384.433	479.178	754.776	2323.090
7	10.113	0.982	543.540	718.722	1292.290	3747.780
8	8.631	0.970	486.952	663.710	1060.890	4117.020
Average	9.361		388.952	486.781	793.976	2597.530
5%						
Sample	Young's Modulus (Pa)	R ²	60% Stress	70% modulus	80% modulus	90% modulus
1	12.211	0.963	463.575	695.591	1511.870	5392.250
2	13.254	0.966	421.914	738.708	1522.960	5611.170
3	8.127	0.952	378.214	677.258	1392.320	4422.510
4	10.255	0.920	433.098	627.685	1232.420	4282.260
5	8.357	0.995	425.324	636.813	1512.510	4979.580
6	10.092	0.917	473.679	677.169	1505.320	5204.410
Average	10.383		432.634	675.537	1446.233	4982.030
7.5%						
Sample	Young's Modulus (Pa)	R ²	60% Stress	70% modulus	80% modulus	90% modulus
1	14.874	0.960	591.167	834.790	1687.750	5266.930
2	8.682	0.986	473.291	626.625	1243.380	4174.920
3	11.646	0.962	525.711	708.230	1260.360	4095.830
4	201.583	0.935	770.284	488.568	504.941	5258.180
5	742.534	0.908	956.927	855.768	469.463	2350.750
6	642.181	0.923	863.167	735.145	325.854	3023.230
Average	270.250		696.758	708.188	915.291	4028.307
10%						
Sample	Young's Modulus (Pa)	R ²	60% Stress	70% modulus	80% modulus	90% modulus
1	688.399	0.940	871.290	625.089	111.432	3230.490
2	728.153	0.969	886.754	628.666	145.789	2993.050
3	679.380	0.921	812.295	541.260	121.108	3246.300
4	187.968	0.955	747.614	444.148	542.901	5395.690
5	229.119	0.955	937.373	526.785	735.851	5715.110
6	341.811	0.934	847.542	559.527	521.004	4474.640
7	289.132	0.960	931.560	576.875	508.860	4615.750
8	277.803	0.938	890.337	668.948	196.510	4039.350
Average	427.721		865.596	571.412	360.432	4213.798

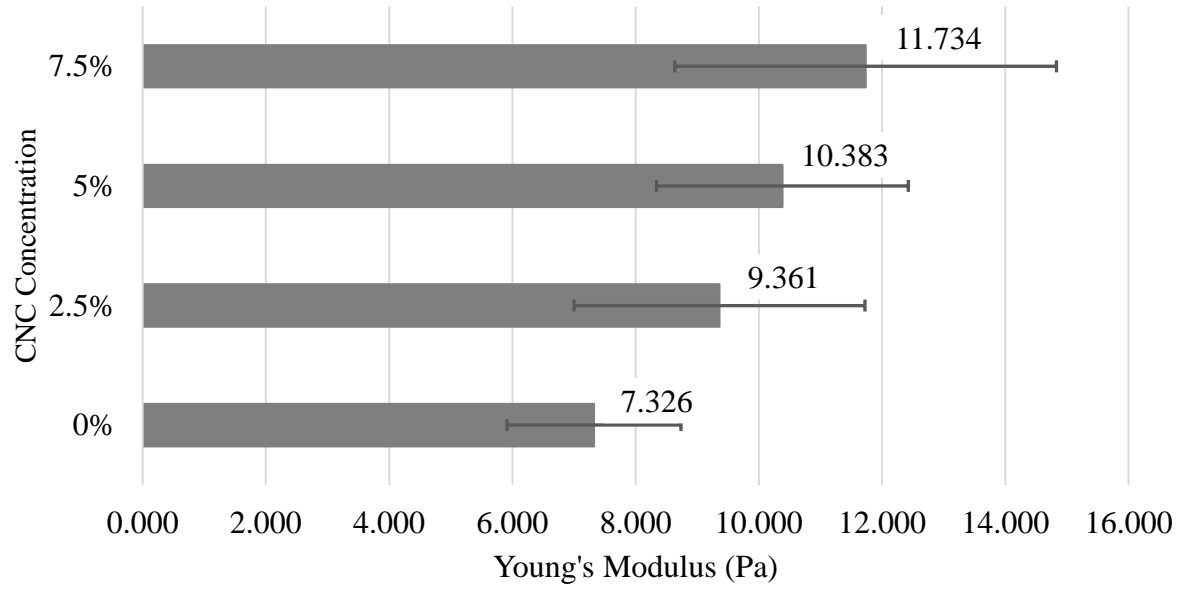


Figure 6: Young's Modulus values for all elastically behaving scaffolds.

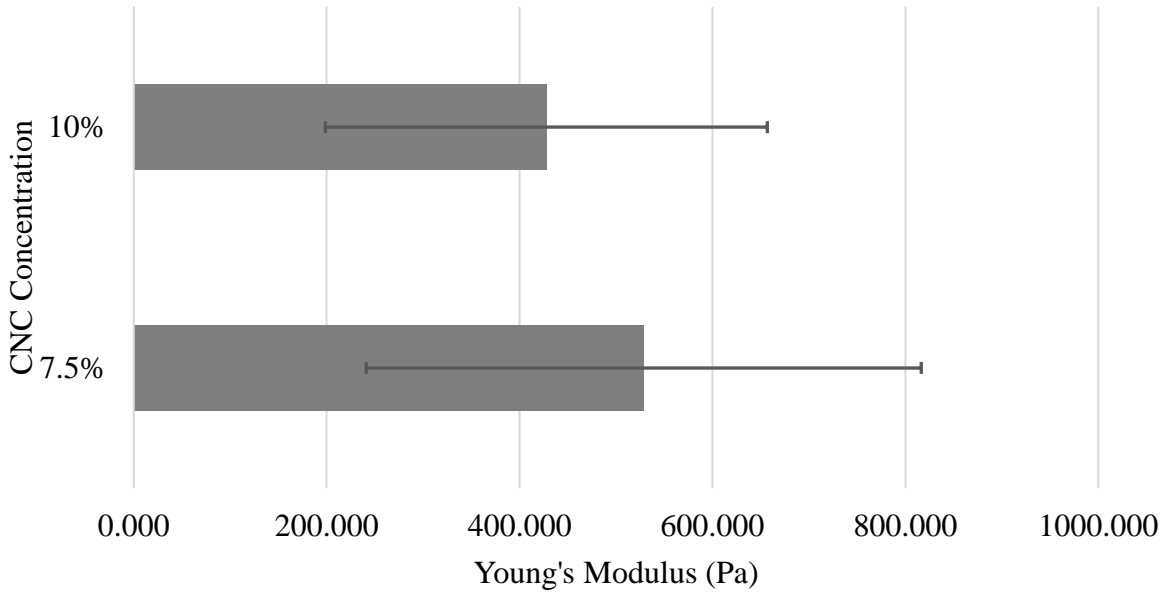


Figure 7: Young's Modulus values for all strain-softening scaffolds.

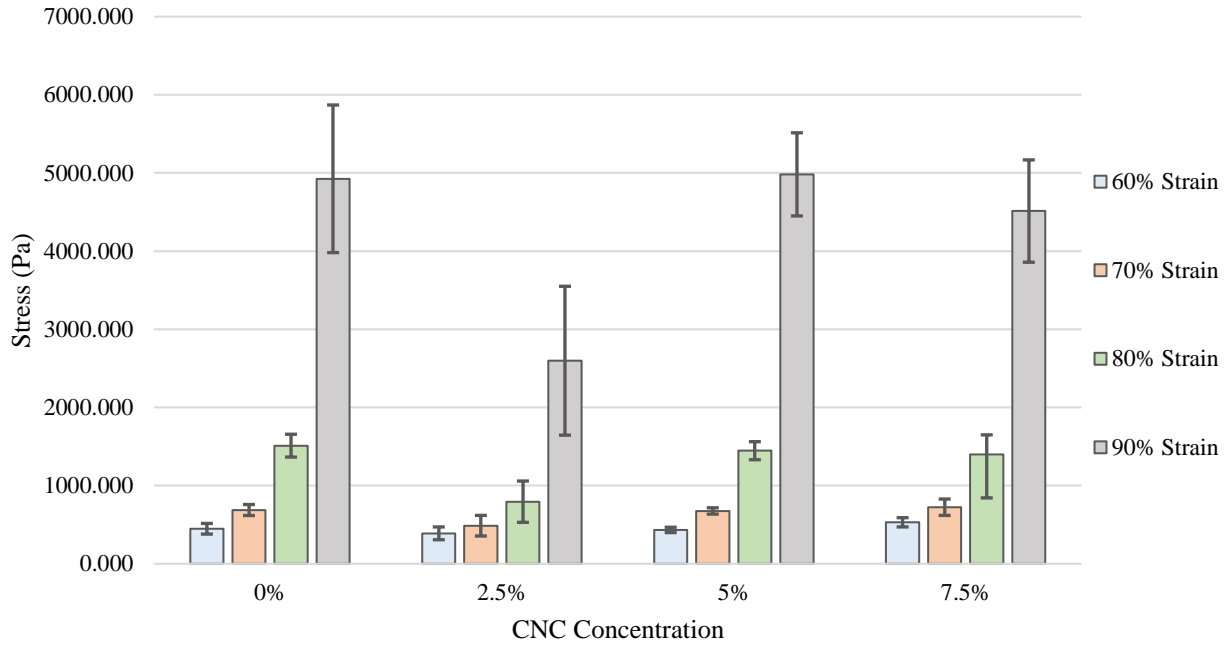


Figure 8: Depicts the mean stress placed on different concentrations of composite gels at various strains for only elastic scaffolds.

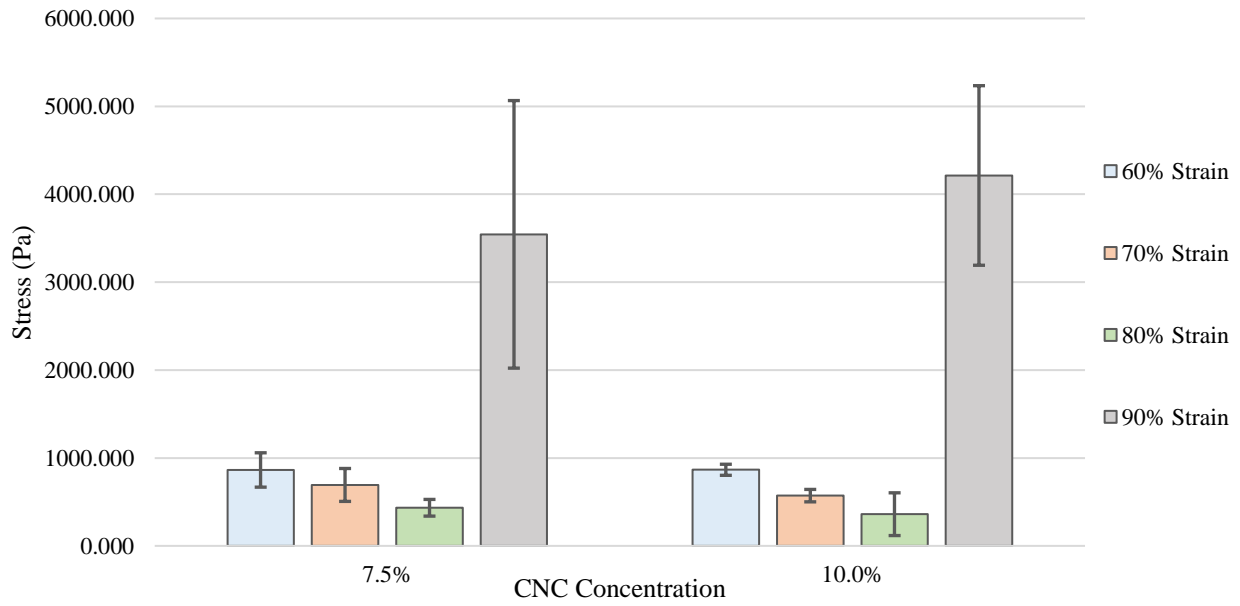


Figure 9: Depicts the mean stress placed on different concentrations of composite gels at various strains for only strain-softening scaffolds.

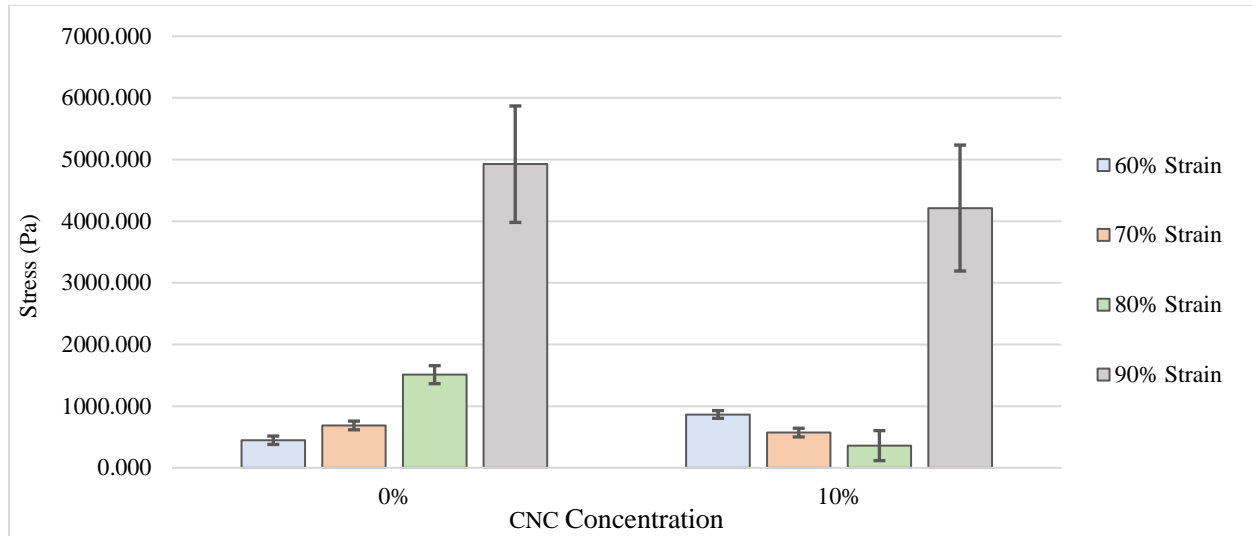


Figure 10: Comparison of 0% and 10% scaffold behaviors.

Table 8: T-test comparing mechanical strength between 7.5% scaffolds and 0% scaffolds.

	7.5%	0%
Mean	11.73406	7.325524
Variance	9.592009467	1.9920471
Observations	3	5
Hypothesized Mean Difference	0	
df	3	
t Stat	2.324876533	
P(T<=t) one-tail	0.051313132	
t Critical one-tail	2.353363435	
P(T<=t) two-tail	0.102626264	
t Critical two-tail	3.182446305	

Table 9: T-test comparing 5-step and 10-step RGB values.

	<i>5-step</i>	<i>10-step</i>
Mean	193.6	221.4
Variance	224.0444	88.26667
Observations	10	10
Hypothesized Mean Difference	0	
df	15	
t Stat	-4.97452	
P(T<=t) one-tail	8.32E-05	
t Critical one-tail	1.75305	
P(T<=t) two-tail	0.000166	
t Critical two-tail	2.13145	

Table 10: T-test comparing 10-step and 15-step RGB values.

	<i>15-step</i>	<i>10-step</i>
Mean	194.7	221.4
Variance	196.2333	88.26667
Observations	10	10
Hypothesized Mean Difference	0	
df	16	
t Stat	-5.00576	
P(T<=t) one-tail	6.47E-05	
t Critical one-tail	1.745884	
P(T<=t) two-tail	0.000129	
t Critical two-tail	2.119905	

Table 11: T-test comparing 2-step and 5-step RGB values.

	<i>5-step</i>	<i>2-step</i>
Mean	193.6	165.4
Variance	224.0444	280.0444
Observations	10	10
Hypothesized Mean Difference	0	
df	18	
t Stat	3.971875	
P(T<=t) one-tail	0.000447	
t Critical one-tail	1.734064	
P(T<=t) two-tail	0.000894	
t Critical two-tail	2.100922	

Table 12: T-test comparing 5-step and 10-step protocols.

	<i>5-step</i>	<i>10-step</i>
Mean	0.291197896	0.1240728
Variance	0.105242114	0.0019746
Observations	3	3
Hypothesized Mean Difference	0	
df	2	
t Stat	0.884038503	
P(T<=t) one-tail	0.23496711	
t Critical one-tail	2.91998558	
P(T<=t) two-tail	0.469934219	
t Critical two-tail	4.30265273	

Table 13: T-test comparing 10-step and 15-step protocols.

	<i>10-step</i>	<i>15-step</i>
Mean	0.124073	0.150933
Variance	0.001975	0.003894
Observations	3	3
Hypothesized Mean Difference	0	
df	4	
t Stat	-0.60731	
P(T<=t) one-tail	0.288217	
t Critical one-tail	2.131847	
P(T<=t) two-tail	0.576435	
t Critical two-tail	2.776445	

Table 14: T-test comparing 5-step and 15-step protocols.

	<i>5-step</i>	<i>15-step</i>
Mean	0.291197896	0.1509326
Variance	0.105242114	0.0038937
Observations	3	3
Hypothesized Mean Difference	0	
df	2	
t Stat	0.735406256	
P(T<=t) one-tail	0.269319878	
t Critical one-tail	2.91998558	
P(T<=t) two-tail	0.538639755	
t Critical two-tail	4.30265273	